

# A Comparative Study of Electrical Transport Phenomena in Ultrathin vs. Nanoscale SOI MOSFETs Devices

A. Karsenty, A. Chelly

**Abstract**—Ultrathin (UTD) and Nanoscale (NSD) SOI-MOSFET devices, sharing a similar W/L but with a channel thickness of 46nm and 1.6nm respectively, were fabricated using a selective “gate recessed” process on the same silicon wafer. The electrical transport characterization at room temperature has shown a large difference between the two kinds of devices and has been interpreted in terms of a huge unexpected series resistance. Electrical characteristics of the Nanoscale device, taken in the linear region, can be analytically derived from the ultrathin device ones. A comparison of the structure and composition of the layers, using advanced techniques such as Focused Ion Beam (FIB) and High Resolution TEM (HRTEM) coupled with Energy Dispersive X-ray Spectroscopy (EDS), contributes an explanation as to the difference of transport between the devices.

**Keywords**—Nanoscale Devices, SOI MOSFET, Analytical Model, Electron Transport.

## I. INTRODUCTION

NANOSCALE Silicon-On-Insulator (SOI) Metal-Oxide-Semiconductor Field-Effect Transistor (MOSFET) based devices are the building blocks of the up-to-date systems allowing ultra-fast data processing. This is in accordance with efforts to develop new generation of ultra-fast computers based on combined electronic and signal processing on one hand [1], and advanced generations of Nanoscale devices for communication systems [2], [3] on the other hand. In this article, a comparative study of the electrical characteristics of two kind of SOI MOSFET's is reported in order to explain the anomalous transport behavior of the thinner one having a channel thickness as low as 1.6 nm and obtained by a selective gate recessed process [4].

## II. EXPERIMENTAL

### A. SIMOX Preferred Wafer Processing Technology

Several techniques were developed in the past to create Silicon-On-Insulator (SOI) devices [5]-[8] since their implementation was found promising [9]-[11] for ULSI [12], low power [13], military and space [14], and cost reducing

A. Karsenty was with the Hebrew University of Jerusalem (HUJI), then with Intel Electronics Corporation, and is now Manager of the Advanced Laboratory of Thin Films' Characterization and Modeling with the Jerusalem College of Technology (JCT), Faculty of Engineering, 21 Havaad Haleumi Street, P.O.B. 16031, Jerusalem, 91160 Israel (phone: 972-2-6751164; fax: 972-2-6751108; e-mail: karsenty@jct.ac.il).

A. Chelly is Manager of the Advanced Semiconductor Devices Lab with Bar-Ilan University (BIU), Faculty of Engineering, Ramat Gan, 52900 Israel (e-mail: chellyr@gmail.com).

[15] applications. Nowadays, SOI wafers are mainly fabricated using the UNIBOND<sup>®</sup> line of SOI wafers and the Smart Cut<sup>®</sup> process technologies, patented by SOITEC Company, allowing excellent thickness uniformity [16]. However, for this research purpose, the former SOITEC technology called Separation-by-IMplanted-Oxygen (SIMOX) was preferred because of the clear advantage of presenting an initial gradient of the SOI thickness across the same wafer. This desirable gradient is conserved during the processing of the Nanoscale devices (NSD). Consequently, it is possible to study the thickness influence on the NSD electrical characteristics.

### B. Buried Oxide Properties

In these SIMOX wafers, the Buried OXide (BOX) is performed by deep implantation of oxygen ions into silicon (p-type with a resistivity of 14–22  $\Omega\cdot\text{cm}$ ), using high energy of 120 keV and dose of  $0.39 \cdot 10^{18}$  ions  $\text{O}^+/\text{cm}^2$ . The ion implantation is performed at a temperature of 600°C for almost two and half hours. Then, an annealing phase of the silicon layer is performed at 1320°C for almost six hours [17]. Of course, change in implant parameters like energy, dose, and temperature may impact the thickness and the interface [18], [19]. The full process resulted in a BOX layer of 70nm under the mono-crystalline silicon (SOI) layer of 53nm. This technology has the advantage of offering an initial silicon thickness gradient that can be preserved during the fabrication process of nanoscale devices.

### C. Thickness Cross-Characterization and Validation

By using a visible light spectrophotometer (FT750) providing multilayer thin films measurements (with layers typical thickness ranges down to 10 nm), the thickness of the SOI layer over the 6” SIMOX wafer was mapped and found varying between 49.83 to 59.40nm [20]. Usage of complementary thin films measurement methods such as ellipsometry, and HRTEM reinforced the thickness results with very high precision. To face the process tooling constraints, 2” diameter wafers had to be cut from the initial 6” SIMOX wafer. The largest thickness gradient zone (located at the opposite edge to the wafer flat) has been selected to be cut. After completing the thinning process (described below) the thickness of the silicon channel was mapped and was found to be varying between 1.64 to 6.57nm.

### D. Furnace Accurate Calibration

The most challenging step was the accurate controlled

thinning process of the SOI layer using local oxidation until reaching a 1.5 – 6.5nm range of thickness (Figs. 1 a and b), while the source and the drain regions remained in their original thickness. To check the capability of accurate thinning, preliminary tests of thinning were performed in order to reach thicknesses lower than 10nm, when characterizing the furnace parameters such as furnace temperature, duration of the oxidation, and growth rate [21].

#### E. Device Processing using Recessed-Gate Channel

The local oxidation was performed by using a nitride mask layer of 38nm (nitride 1) grown on a thin oxide layer (PAD OX) of 15nm. The role of the pad oxide was to serve as an interface between the nitride and the silicon in order to prevent mechanical stresses. A first etching of the nitride and pad oxide layer at the extremities of the active region allowed their oxidation into a 700nm thick Field Oxide (FOX). A second etching, performed in the center of the nitride region, allowed an exposure of the channel region while the surrounding nitride capped the source and drain areas. Two steps of oxidation were then performed: First, a 75nm thick sacrificial oxide layer, called Channel Oxide (CHAN OX) was grown in order to decrease the channel thickness to about 10nm in a more significant way, and then was finally removed. The second phase of the oxidation (26 nm thick), called Gate Oxidation (GOX), was a more accurate step allowing to reach the final Nanoscale thickness of the channel, in the range of 1.6nm to 6.5nm, and serving as the Gate Oxide itself, when the thickness distribution uniformity and the Si-SiO<sub>2</sub> interface quality [22] are serving as important parameters [23], [24]. In order to get reference devices on the same wafer, i.e. having an initial silicon channel close to 46 nm, the nitride mask was not etched so the gate insulator layer remained 38 nm thick nitride layer deposited on the 15nm PAD OX layer.

#### F. Contact Electrodes' Fabrication

A polycrystalline silicon layer of 220nm was deposited over the gate oxide, then oxidized, and patterned to form the gate electrode. Before the source/drain/gate phosphorus implant, a thin layer nitride (nitride 2) of 30nm was deposited in order to prevent further oxidation of the thin silicon layer during the implant's thermal annealing. A Plasma Enhanced Chemical Vapor Deposition (PECVD) oxide (Silox 2) of 350nm thickness was deposited followed by the aluminum metallization step to define the contact areas.

#### G. Electrical Transport Measurements' Set-Up

The I-V Characteristics' measurements (room temperature, dark conditions) were performed using the Semiconductor Characterization System (SCS-4200) from Keithley Ltd. The Devices Under Test (DUT) were packaged on a 24-DIP ceramic chip carrier and mounted on a commercial triax test fixture (Keithley model 8600) allowing a connection of up to four devices at a time.

### III. RESULTS AND DISCUSSION

#### A. Structural Characterization

Both representative SOI MOSFET devices having a same ratio W/L of 80/8 (μm) were analyzed using FIB and HRTEM techniques. A FIB cross-section of the Ultrathin Device (UTD) (46nm channel thick) is presented in Fig. 1 showing the device structure (Fig. 1 a) and the morphology of the layers forming the gate region (Fig. 1 b). A HRTEM zoom-in of the recessed silicon channel for the Nanoscale Device (NSD) is presented in Fig. 2, confirming the 1.6nm thickness value.

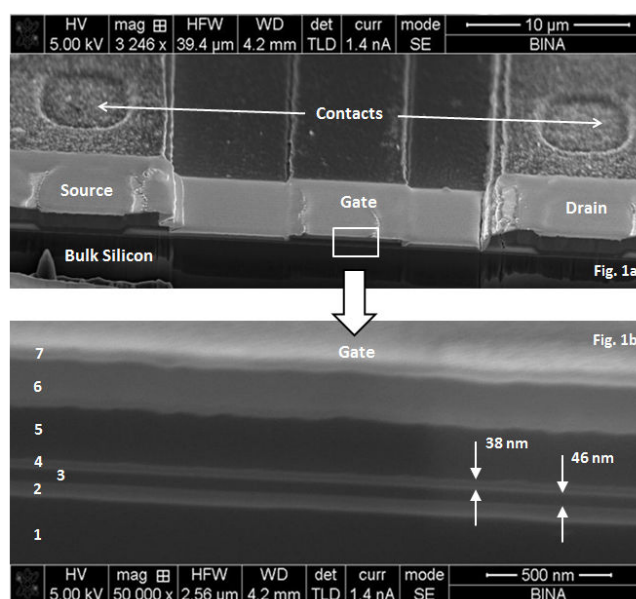


Fig. 1 a) FIB cross-section of the Ultrathin Device (UTD) (46nm channel thickness) showing the device structure including the source, gate and drain regions. b) Zoom in of the layers below the gate region: 1. Bulk silicon, 2. Buried oxide, 3. Silicon channel, 4. Nitride1/Gate Oxide, 5. Polysilicon, 6. Silox2/Nitride2, and 7. FIB metal deposition.

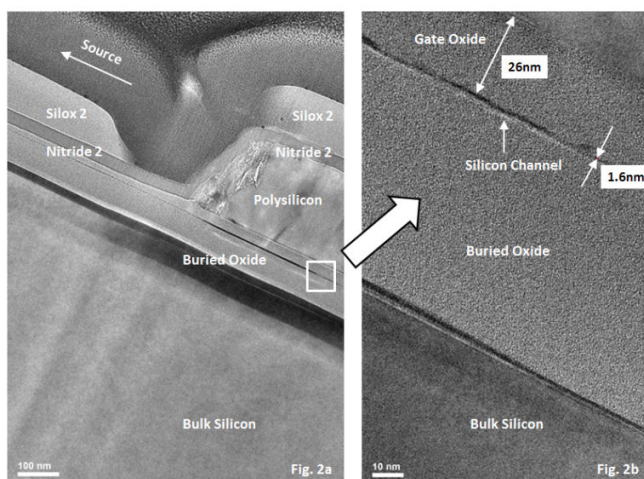


Fig. 2 a) HRTEM image of Nanoscale Device (NSD), showing a view of the gate's edge away from the source contact. Since the edge of the source is located 10 $\mu$ m away from the Gate's edge, the source is not visible here. b) Zoom in below the Gate region reveals details of the recessed Silicon Channel and confirms the 1.6nm thickness value. Gate oxide thickness is 26 nm.

### B. Electrical Characterization and Model

In Fig. 3 are presented the  $I_{DS}$ - $V_{GS}$  measured characteristics (semi log scale) of the UTD when compared to the NSD's (solid lines).  $V_{DS}$  is kept constant to 0.4V which is close to the limit of the linear operation domain of the device [20].

Starting with UTD characteristic, it can be observed that for  $V_{GS}$  values more negative than -0.8 V,  $I_{DS}$  is slowly decreasing, and indicating a leakage phenomenon (negative resistance) similar to the Gate Induced Drain Leakage (GIDL) observed for both classic and SOI-MOSFET devices [25]. The same leakage phenomenon and amplitude are also measured for the NSD showing that the leakage is almost independent of the channel thickness as expected. Above -0.8 V the UTD characteristic is exponential (sub threshold region) with a relatively high swing value of 115 mV/dec ("ideal" value is  $\ln(10)kt/q=60$  mV/dec at room temperature). The threshold voltage  $V_T$  of the UTD is evaluated to -0.4V as extrapolated from the linear part of the  $I_{DS}$ - $V_{GS}$  graph (not shown here). The effective mobility is derived from the dependence of the channel conductance  $g_d$  (as measured from  $I_{DS}$ - $V_{DS}$  characteristics not presented here) on  $V_{GS}$ - $V_T$  in the linear domain according to (1):

$$\mu_{eff} = \frac{g_d L}{WC_{gate}(V_{GS} - V_T)} \quad (1)$$

In UTD, the gate insulator is composed of a thin oxide layer (PAD OX) of 15nm thick and a nitride protective layer (again the recess oxidation process) of 38nm thick. Consequently, the gate capacitance  $C_{gate}$  is estimated to 121 nF/cm<sup>2</sup> and the Equivalent Oxide Thickness (EOT) is 28nm which is close to the NSD gate oxide thickness (25nm) as seen in Fig. 2 b). According to (1),  $\mu_{eff}$  is decreasing from 1380 cm<sup>2</sup>/Vs to 630 cm<sup>2</sup>/Vs by increasing  $V_{GS}$  from 0 to 4V. The values are

consistent with those obtained for similar SOI MOSFET devices [26]-[28].

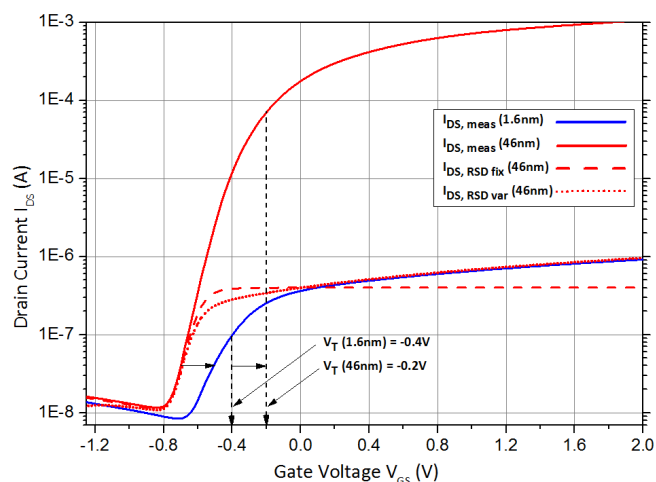


Fig. 3  $I_{DS}$ - $V_{GS}$  (semi-log) characteristics for Ultrathin Device (UTD) (46nm) and Nanoscale Device (NSD) (1.6nm) for  $V_{DS} = 0.4V$ .

As for the NSD characteristic, presented in Fig. 3 (solid line), above a  $V_{GS}$  value of -0.6V,  $I_{DS}$  is growing steeply in an exponential trend until -0.3V (subthreshold domain). The swing value is found surprisingly high (230 mV/dec) when compared to the previous UTD's value and also when compared to similar devices [29]. This result reveals an unexpected degradation of the subthreshold conduction correlated to the thinning process.

Another interesting fact noticed in Fig. 3, is that the subthreshold domain of the NSD is positively shifted by 0.2V relatively to the UTD device. Consequently, the NSD threshold voltage can be estimated to -0.2V. This result is consistent with the increasing of  $V_T$  in a comparable amount by thinning the channel below 10nm due to quantum mechanics considerations [30].

For positive  $V_{GS}$  values, the characteristic is bent and turned into a linear dependence on  $V_{GS}$ . Surprisingly,  $I_{DS}$  is measured to be three orders of magnitude lower than the UTD in the same region. Since the effective mobility ( $\mu_{eff}$ ) is limited to a minimum value of about 100-200 cm<sup>2</sup>/Vs in Nanoscale SOI-MOSFET [31], [32] devices, the mobility variation as a function of the channel thickness cannot explain such a huge conductance attenuation. These characteristics are interpreted as resulting from the influence of a huge parasitic drain-source series resistance coupled with a gate leakage current that overwhelm the intrinsic channel resistance. The intercept value of  $I_{DS}$  at zero  $V_{GS}$  is about 0.4  $\mu$ A for a  $V_{DS}$  value of 0.4 V. Assuming that  $V_{DS}$  value is only dropped by a series total resistance ( $R_{SD}=R_S+R_D$ ), the  $R_{SD}$  value results in 1 M $\Omega$ . Varying  $V_{DS}$  had shown a linear dependence of  $I_{DS}$  with  $V_{DS}$  at zero  $V_{GS}$  confirming the assumption [20].

The influence of a series resistance  $R_{SD}$  on the drain current in the linear domain can be described by the following equation [33]:

$$\text{For } V_{GS} \geq V_T, I_{DS,lin} = \left( \frac{g_d}{1 + g_d R_{SD}} \right) V_{DS} \quad (2)$$

Using (2), a calculation can be done for the UTD's characteristic, disturbed by a fixed series resistance  $R_{SD}$  from the measured characteristic  $I_{DS, meas}$ , and according to the following expression:

$$I_{DS,R_{SD}fix} = \frac{I_{DS,meas}}{1 + I_{DS,meas} \frac{R_{SD}}{V_{DS}}} \quad (3)$$

In Fig. 3, is presented the  $I_{DS}$ - $V_{GS}$  characteristic (dashed line) of the UTD disturbed by a fixed series resistance  $R_{SD}$  of 1 M $\Omega$  according (3).

Indeed, (3) is equivalent to (2) in the linear domain (above -0.4 V) and is still valid in the subthreshold domain (below -0.4 V) since  $I_{DS, meas}$  become negligible relative to  $V_{DS} / R_{SD}$  i.e. 0.4 $\mu$ A. The calculated  $I_{DS,R_{SD}fix} - V_{GS}$  characteristic (dashed line) fits the NSD characteristic within the same order of magnitude but with a shift of -0.2V attributed to the difference of threshold voltage between the devices as mentioned above. However, for positive  $V_{GS}$ , the disturbed characteristic is a constant and then cannot fit the linear variation of  $I_{DS}$ .

In order to interpret this linear trend, a decrease of  $R_{SD}$  with  $V_{GS}$  can be considered, as observed in MOSFET's [34], according to:

$$R_{SD} = \frac{R_{SD0}}{1 + \theta V_{GS}} \quad (4)$$

In our NSD case,  $R_{SD}$  is 1 M $\Omega$  as mentioned above and  $\theta$  was estimated to 0.70 [20].

Then, the calculated characteristic of the UTD disturbed by a variable series resistance  $R_{SD}$  can be re-written as:

$$I_{DS,R_{SD},var} = \frac{I_{DS,meas}}{1 + I_{DS,meas} \frac{R_{SD0}}{(1 + \theta V_{GS}) V_{DS}}} \quad (5)$$

In Fig. 3, it is presented that the recalculated  $I_{DS, R_{SD} var}$  characteristic (dotted line), evaluated from (5), gave the best fit to the NSD characteristic. This helps to conclude that the characteristics of the NSD can be derived from the UTD by introducing a huge gate-controlled series resistance and by a positive shift of the threshold voltage.

#### IV. PHYSICAL INTERPRETATION OF THE ELECTRICAL MODEL

Based on geometrical considerations, the difference of silicon channel thicknesses (factor 30) cannot in itself explain the difference in more than three orders of magnitude in the drain current. Secondly, phenomena that usually increase the spreading resistance, like the gradient of dopant concentration near the silicon channel extensions [34] and a gate mask mismatch, are not found relevant enough to explain the

difference. But, as seen on Fig. 4, the gate-recessed process used to thin the channel has also squeezed the channel extensions located far from the gate region. Moreover, an Energy Dispersive X-ray Spectroscopy (EDS) was performed. It provides a local elemental analysis of the regions near the gate edge (EDS2) and further away (EDS3) in the source direction. It turns out that the later region (EDS3) still appears rich in oxygen (Si/O=2.5) and is comparable to the gate edge region (EDS2, Si/O=1.74). This over oxidation of the channel extensions can explain the apparition of a high series resistance.

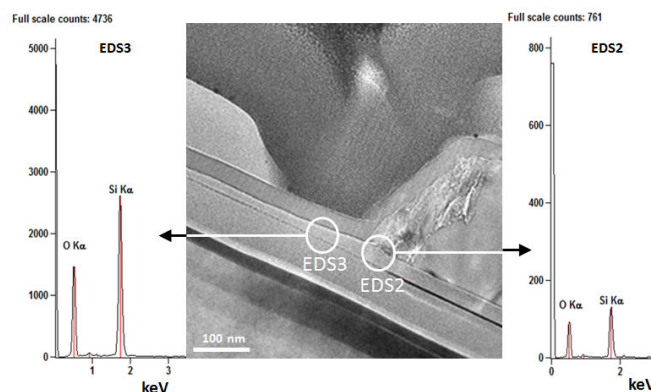


Fig. 4 EDS graphs representing the atomic concentration peaks of Silicon and Oxygen at two sites near the gate edge as shown on the corresponding HRTEM picture

#### V. CONCLUSIONS

Nanoscale SOI MOSFET devices were fabricated using a selective recess gate thinning process. I-V characteristics are measured and compared for the same W/L ratio to Ultrathin SOI MOSFET devices (non recess gate thinned). An abnormality of electrical transport (attenuation by three orders of magnitude of the drain current) is observed in the linear region for the Nanoscale device having a channel thickness as low as 1.6nm relative to the ultrathin device (46 nm channel thick). This result is interpreted and modeled analytically by introducing a huge gate controlled drain-source series resistance in the characteristics of the ultrathin device. This resistance seems to be due to an over oxidation of the channel extensions during the thinning process. The added value of this study is to provide an interpretative approach for modern Nanoscale devices, presenting disturbed electrical characteristics (high series resistance, mobility reduction, leakage current...), and which could be useful for prediction of transport phenomena at the Nanoscale.

#### REFERENCES

- [1] D. Esseni, P. Palestri and L. Selmi, "Nanoscale MOS transistors, semiclassical transport and applications", Cambridge University Press, 2011.
- [2] A. Karsenty, A. Sa'ar, N. Ben-Yosef, and J. Shappir, "Enhanced electroluminescence in silicon-on-insulator metal-oxide-semiconductor transistors with thin silicon layer", *Appl. Phys. Lett.*, 82, 4830 (2003).
- [3] D. Abraham, A. Chelly, D. Elbaz, S. Schiff, M. Nabozny, and Z. Zalevsky, "Modeling of Current-Voltage Characteristics of the Photoactivated Device Based on SOI Technology", *Active and Passive Electronic Components*, vol. 2012, Article ID 276145, 7 pages, 2012.

- [4] M. Chan, F. Assaderaghi, S. A. Parke, S. S. Yuen, C. Hu, and P. K. Ko, "Recess channel structure for reducing source/drain series resistance in ultra-thin SOI MOSFETs", *Proc. IEEE Int. SOI Conf.*, Oct. 1993, pp. 172-173.
- [5] S. Cristoloveanu and S. S. Li, "Methods of Forming SOI Wafers - Electrical Characterization of S.O.I. Material and Devices", Kluwer Academic Publishers, Chapter 2, p. 7-15, 1995.
- [6] S. Cristoloveanu, Status, "Trends and Challenges of Silicon-on-Insulator Technology - SOI: A Metamorphosis of Silicon", *IEEE Circuits & Devices*, p. 26-32, January 1999.
- [7] M. Bruel, B. Aspar, B. Charlet, C. Maleville, T. Poumeyrol, A. Soubie, A.-J. Auberton-Herve, J. M. Lamure, T. Barge, F. Metral, and S. Trucchi, "SMART CUT: A Promising New SOI Material Technology", *Proceedings 1995 IEEE International Conference*, p. 178-179, October 1995.
- [8] B. Dance, "European SOI Comes of Age, Semiconductor International", p. 83-90, November 1994.
- [9] L. Peters, "SOI Takes Over Where Silicon Leaves Off", *Semiconductor International*, March 1993.
- [10] M. Alles and S. Wilson, "Thin Film Silicon on Insulator: An Enabling Technology", *Semiconductor International*, April 1997.
- [11] A. J. Auberton-Herve and Tadashi Nishimura, "SOI-based devices: Status Overview", *Solid State Technology*, July 1994.
- [12] A. J. Auberton-Herve, J. M. Lamure, T. Barge, M. Bruel, B. Aspar, and J. L. Pelloie, "SOI Materials for ULSI Applications", *Semiconductor International*, p.97-104, October 1995.
- [13] T. E. Thompson, "SOI sandwich promises fast, low-power ICs", *Electronic Business Today*, p. 43-47, October 1995.
- [14] J. Rhea, "DARPA low power program aims at mobile applications", *Military & Aerospace Electronics*, July 1996.
- [15] P. H. Singer, "U. S. Chipmakers: Penny-Wise, Million-Dollar Foolish", *Semiconductor International*, August 1995.
- [16] M. Bruel, B. Aspar, B. Charlet, C. Maleville, T. Poumeyrol, A. Soubie, A.-J. Auberton-Herve, J. M. Lamure, T. Barge, F. Metral, and S. Trucchi, "SMART CUT<sup>®</sup>: A Promising New SOI Material Technology", *Proceedings 1995 IEEE International Conference*, p. 178-179, October 1995.
- [17] B. Aspar, C. Pudda, A. M. Papon, A.J. Auberton-Herve, and J. M. Lamure, "Ultra-thin buried oxide layers formed by low dose SIMOX processes", *The Electrochemical Society: proceedings*, Vol. 94, No. 11, p. 62, abstract 541 Silicon On Insulator Technology and Devices edited by S. Cristoloveanu.
- [18] R. Datta, L. P. Allen, R. P. Dolan, K. S. Jones, and M. Farley, "Independent implant parameter effects on SIMOX SOI dislocation formation", *Materials Science & Engineering B*, Vol. 46, Elsevier Science publications p. 8-13, 1997.
- [19] V. V. Afanas'ev, G. A. Brown, H. L. Hughes, S. T. Liu, and A. G. Revesz, "Conducting and Charge-Trapping Defects in Buried Oxide Layers of SIMOX Structures", *J. Electrochem. Soc.*, Vol. 143, No. 1, p. 347-352, January 1996.
- [20] A. Karsenty, A. Chelly, "Modeling the Transfer Characteristics for High Series Resistance Nanoscale Silicon-On-Insulator (SOI) MOSFETs", *Appl. Phys. Lett.*, submitted for publication.
- [21] A. Karsenty, "Study of the Electrical and Electro-Optical Phenomena in Thin SOI MOS Transistors", *PhD Thesis*, Hebrew University Of Jerusalem, May 2003.
- [22] L. Do Thanh and P. Balk, "Elimination and Generation of Si-SiO<sub>2</sub> Interface Traps by Low Temperature Hydrogen Annealing", *J. Electrochem. Soc.*, Vol. 135, No. 7, p. 1797-1801, July 1988.
- [23] S. Cristoloveanu and T. Ouisse, "The Physics and Chemistry of SiO<sub>2</sub> and the Si-SiO<sub>2</sub> Interface 2", edited by C.R. Helms and B.E. Deal Plenum Press New York, p. 309-318, 1993.
- [24] V. V. Afanas'ev, A. G. Revesz, and H. L. Hughes, "Confinement Phenomena in Buried Oxides of SIMOX Structures as Affected by Processing", *J. Electrochem. Soc.*, Vol. 143, No. 2, p. 695-700, February 1996.
- [25] J. Wan, C. Le Royer, A. Zaslavsky, S. Cristoloveanu, "Gate-induced drain leakage in FD-SOI devices: What the TFET teaches us about the MOSFET", *Microelectronic Engineering*, Volume 88, issue 7, July 2011, Pages 1301-1304.
- [26] J. Wang, N. Kistler, J. Woo, and C. R. Viswanathan, "Mobility-field behavior of fully depleted SOI MOSFETs", *IEEE Electron Device Lett.* 15, 117 (1994).
- [27] D. Esseni, M. Mastrapasqua, G.K. Celler, C. Fiegna, L. Selmi, and E. Sangiorgi, "Low field electron and hole mobility of SOI transistors fabricated on ultrathin silicon films for deep submicrometer technology application", *IEEE Electron Device Lett.* 48, 2842 (2001).
- [28] K. Uchida and S. Takagi, "Carrier scattering induced by thickness fluctuation of silicon-on-insulator film in ultrathin-body metal-oxide-semiconductor field-effect transistors", *Appl. Phys. Lett.* 82, 2916 (2003).
- [29] T. Ernst, S. Cristoloveanu, G. Ghibaudo, T. Ouisse, S. Horiguchi, Y. Ono, Y. Takahashi and K. Murase, "Ultimately thin double-gate SOI MOSFETs", *IEEE Trans. Electron Devices* ED-50, 3 (2003).
- [30] Y. Omura, S. Horiguchi, M. Tabe and K. Kishi, "Quantum-Mechanical Effects on the Threshold Voltage of Ultrathin-SOI nMOSFET's", *IEEE Electron Device Lett.* 14, 569 (1993).
- [31] J. H. Choi, Y.J. Park and H.S. Min, "Electron mobility behavior in extremely thin SOI technology with MOSFETs", *IEEE Electron Device Lett.* 16, 527 (1995).
- [32] M. Schmidt, M.C. Lemm, H.D.B. Gottlob, F. Driussi, L.Selmi and H. Kurz, "Mobility extraction in SOI MOSFETs with sub 1 nm body thickness", *Solid State Electronics* 53, 1246 (2009).
- [33] K. Lee, M. Shur and T. A. Fjeldly, "Semiconductor device modeling for VLSI", Prentice Hall 244 (1993).
- [34] K. K. NG and W. T. Lynch, "Analysis of the gate-voltage-dependent series resistance of MOSFETs", *IEEE Trans. Electron Devices* ED-33, 7 (1986).



**A. Karsenty** was born in France in 1965. He emigrated from France to Israel in 1983, and received the Engineering and BSc Degree in Physics/Electro-Optics Department from the *Jerusalem College of Technology (JCT)* in 1989. Pursuing Research (Eshkol Grant) at the *Fredy & Nadine Hermann Graduate School of Applied Science*, he received the MSc Degree in Applied Physics & Material Science (Microelectronics & Electro-Optics Divisions) from the *Hebrew University of Jerusalem (HUJI)*, Israel in 1996, and the PhD Degree in Applied Physics & Material Science (Microelectronics & Electro-Optics Divisions), from the *Hebrew University of Jerusalem (HUJI)*, Israel in 2003. His main fields of study are Quantum Well Devices Modeling, Nanofabrication and Nanocharacterization, as well as Quality & Reliability Engineering of Devices.

He worked more than 22 years in High-Tech industries, in Europe and Israel, part of which as Senior Engineer and Manager for 16 years (1995-2011) with Intel Electronics Corporation. In 2011, he joined the *Jerusalem College of Technology (JCT)* where he is in the process of founding a Nanotechnology Center and manages the Thin Film Characterization and Modeling Advanced Laboratory. He is leading research on nanoscale electro-optics devices.

Dr. A. Karsenty is IEEE Member, IEF (Israeli Engineering Federation) Member, and received more than 30 Awards in Engineering and Physics.



**A. Chelly** was born in France in 1969. He received the MSc. degree (*Magistere*) in Material science from the *Universite Louis Pasteur (ULP)*, Strasbourg, France, in 1992 and the Ph.D. degree in Solid State Physics from the *Universite de Haute Alsace (UHA)*, Mulhouse, France, in 1997 on the epitaxial growth of SiGe layers on silicon from gas sources. He emigrated from France to Israel in 1997 and held a Postdoctoral position (Eshkol Grant) at the *Fredy & Nadine Hermann Graduate School of Applied Science* of the Hebrew University of Jerusalem, Israel. He was involved in the development and fabrication of silicon nano-detector for microscopy in near-field optics. Then, he continued to work as a research engineer at the Microelectronics Laboratory till 2004 on processing of neuronal chip in the framework of the European consortium. Then, He moved to *Bar Ilan University (BIU)*, Israel, where he established the Advanced Semiconductor Devices Laboratory at the Faculty of Engineering. He is giving lectures on Semiconductor Processing and Advanced Semiconductor devices. Dr. Chelly is involved in research on electro-optics and nano-scale electronic devices.